

UC Davis

UC Davis Previously Published Works

Title

Post-traumatic osteoarthritis progression is diminished by early mechanical unloading and anti-inflammatory treatment in mice

Permalink

<https://escholarship.org/uc/item/5t8105t4>

Journal

Osteoarthritis and Cartilage, 29(12)

ISSN

1063-4584

Authors

Hsia, AW
Jbeily, EH
Mendez, ME
[et al.](#)

Publication Date

2021-12-01

DOI

10.1016/j.joca.2021.09.014

Peer reviewed



Published in final edited form as:

Osteoarthritis Cartilage. 2021 December ; 29(12): 1709–1719. doi:10.1016/j.joca.2021.09.014.

Post-Traumatic Osteoarthritis Progression is Diminished by Early Mechanical Unloading and Anti-Inflammatory Treatment in Mice

Allison W. Hsia¹, Elias H. Jbeily¹, Melanie E. Mendez², Hailey C. Cunningham¹, Kristin K. Biris¹, Heejung Bang³, Cassandra A. Lee¹, Gabriela G. Loots², Blaine A. Christiansen¹

¹:University of California Davis Health, Department of Orthopaedic Surgery, Lawrence J. Ellison Musculoskeletal Research Center, 4635 2nd Ave, Suite 2000, Sacramento, CA 95817

²:Lawrence Livermore National Laboratory, Physical and Life Sciences Directorate, 7000 East Avenue, L-452, Livermore, CA 94550

³:University of California Davis Health, Department of Public Health Sciences, Sciences 1C, Suite 145, Davis, CA 95616

Abstract

Objective: Post-traumatic osteoarthritis (PTOA) is a degenerative joint disease initiated by injury. Early phase (0–7 days) treatments often include rest (unloading) and anti-inflammatory medications, but how those early interventions impact PTOA progression is unknown. We hypothesized that early unloading and anti-inflammatory treatment would diminish joint inflammation and slow PTOA progression.

Design: Mice were injured with non-invasive ACL rupture followed by hindlimb unloading (HLU) or normal cage activity (ground control: GC) for 7 days, after which all mice were allowed normal cage activity. HLU and GC mice were treated with daily celecoxib (CXB; 10 mg/kg IP) or vehicle. Protease activity was evaluated using *in vivo* fluorescence imaging, osteophyte formation and epiphyseal trabecular bone were quantified using micro-computed tomography, and synovitis and articular cartilage were evaluated using whole-joint histology at 7, 14, 21, and 28 days post-injury.

Corresponding Author: Blaine A. Christiansen, University of California Davis Health, Department of Orthopaedic Surgery, Lawrence J. Ellison Musculoskeletal Research Center, 4635 2nd Ave, Suite 2000, Sacramento, CA 95817, *Phone:* 916-734-3974, *bchristiansen@ucdavis.edu*.

Author Contributions:

AWH was primarily responsible for all sample and data collection, data analysis, study design, and manuscript writing. EHJ conducted microCT analysis and grading/evaluation of histological sections. MEM performed processing, staining, and evaluation of histological sections. HCC performed data analysis and generated figures. KKB conducted grading and evaluation of histological sections. HB performed statistical analysis, group size calculations, and helped generate tables. CAL provided clinical perspective, and consulted on study design, interpretation of results, and manuscript writing. GGL assisted with study design, oversight and guidance of experimental procedures, and contributed to manuscript writing. BAC coordinated all analyses, assisted with study design and interpretation of results, and contributed to manuscript writing.

Publisher's Disclaimer: This is a PDF file of an unedited manuscript that has been accepted for publication. As a service to our customers we are providing this early version of the manuscript. The manuscript will undergo copyediting, typesetting, and review of the resulting proof before it is published in its final form. Please note that during the production process errors may be discovered which could affect the content, and all legal disclaimers that apply to the journal pertain.

Conflict of Interest:

The authors have no conflicts of interest to disclose.

Results: HLU significantly reduced protease activity (–22–30% compared to GC) and synovitis (–24–50% relative to GC) at day 7 post-injury (during unloading), but these differences were not maintained at later timepoints. Similarly, trabecular bone volume was partially preserved in HLU mice at during unloading (–14–15% BV/TV for HLU mice, –21–22% for GC mice relative to uninjured), but these differences were not maintained during reloading. Osteophyte volume was reduced by both HLU and CXB, but there was not an additive effect of these treatments (HLU: –46%, CXB: –30%, HLU+CXB: –35% relative to vehicle GC at day 28).

Conclusions: These data suggest that early unloading following joint injury can reduce inflammation and potentially slow PTOA progression.

Introduction

Post-traumatic osteoarthritis (PTOA) affects over 5 million people in the United States [1, 2]. PTOA is a degenerative joint disease that occurs after a traumatic joint injury such as anterior cruciate ligament (ACL) rupture [3–5], injury to the meniscus [6, 7] or articular cartilage [8], and intra-articular fracture [9, 10]. PTOA affects all joint tissues and leads to osteophyte development [11], and joint degeneration may lead to severe pain and disability. Despite the prevalence of PTOA, little is understood about many of the factors that contribute to the disease, or how current standard-of-care following a joint injury impacts PTOA progression.

Injury initiates an inflammatory response that includes the release of proteases and cytokines that contribute to joint degeneration [12]. Injury also produces mechanical changes in the joint (i.e., joint instability) that may lead to cartilage degeneration through altered mechanical loading, and can aggravate injured joint tissues and exacerbate the inflammatory response. The current clinical standard-of-care in the early stage (1–2 weeks) after joint injury in human patients aims to reduce inflammation through decreased mechanical loading (rest or low-level activity) and the administration of non-steroidal anti-inflammatory drugs (NSAIDs). While these treatments are effective for reducing swelling and pain after injury, the long-term effects of these early interventions on PTOA progression is unclear.

Previously, we showed that hindlimb unloading (HLU) following ACL injury in mice reduced protease activity in the joint and diminished osteophyte development [13]. Similarly, hindlimb immobilization in guinea pigs after intra-articular injection of iodoacetate completely prevented osteophyte formation, led to a reduction in osteophyte size with subsequent remobilization, and mitigated the degenerative changes found during OA [14–16]. Additionally, hindlimb immobilization in beagles led to reduced synovial fluid levels of interleukin-1 α , tissue inhibitor of metalloproteinases 1 (TIMP-1), and chondroitin sulfate [17]. However, while these studies investigated the effect of unloading on joint health, most patients return to relatively normal levels of physical activity after a period of rest following a joint injury. Few studies have examined the effects of reloading after a period of unloading [18]. Previous studies have employed animal models of immobility to examine the effects of normal ambulation or running post-immobilization [14, 16, 19]. However, not all of these studies were performed in the context of joint injury, and most examined a limited number of time points after remobilization. Additionally, immobilization

is not a clinically relevant model for examining rest after ACL injury, as most patients undergo at least some amount of passive mobility after injury.

Previous studies were also limited because they did not investigate the effect of unloading in combination with NSAIDs, which may have a synergistic effect in reducing PTOA development. Celecoxib (CXB), a selective inhibitor of cyclooxygenase 2 (COX-2) that is currently used as an analgesic for OA patients, may potentially modulate disease progression when used in the early stage following a joint injury. In preclinical studies, CXB was shown to affect many tissues involved in OA pathogenesis, including articular cartilage, bone, and synovium [20]. For example, in mice with collagen-induced arthritis (CIA), CXB treatment suppressed bone resorption and loss of trabecular bone mass and inhibited IL-6 expression in synovial tissue [21]. In another study using CIA in mice, combined treatment with CXB and cilostazol was able to reduce hindlimb paw thicknesses, cartilage depletion, serum IL-1 β levels, and bone erosion, and increase serum IL-10 levels [22]. Similarly, treatment with a COX-2 inhibitor was able to prevent subchondral bone changes and attenuate cartilage degeneration in STR/Ort mice (an established model of spontaneous OA), as well as tumor necrosis factor- α transgenic mice (a model of rheumatoid arthritis) [23]. In a rat ACL transection model of OA, controlled intra-articular delivery of CXB reduced osteophyte formation, subchondral sclerosis, bone cysts, and synovial inflammation [24].

In the current study, we used a noninvasive mouse model of ACL rupture to determine the therapeutic efficacy of early unloading (rest) in combination with CXB treatment in reducing long-term PTOA progression. We hypothesized that 1) CXB treatment and early unloading would each individually reduce inflammation, inhibit osteophyte formation, and diminish PTOA progression, and would have an additive therapeutic effect when used simultaneously; and 2) osteophyte formation and PTOA progression will resume during reloading, but will remain diminished compared to mice that did not undergo an unloading period.

Methods

Animals

One hundred and sixteen skeletally mature (12-weeks-old at injury [25]) female C57BL/6 mice were obtained from The Jackson Laboratory (Sacramento, CA) and were acclimated for 1–2 weeks before injury (Fig. 1). Mice were randomly assigned to experimental groups. Mice were subjected to non-invasive ACL rupture or sham injury as previously described [26]. Mice were allowed to either ambulate freely (ground control, GC) or immediately underwent hindlimb unloading (HLU) for 7 days prior to reloading (n=6–7/group). Group sizes were based on our previous study that used hindlimb unloading in mice following non-invasive knee injury [27]. Based on data from this previous study, 4–8 mice per group would provide sufficient power to detect similar effect sizes with 80% power, under 5% alpha, where n=7–8 is assuming conservative standard deviation and n=4 is assuming averaged standard deviation. Mice were treated daily with either 10 mg/kg Celecoxib (CXB; Selleckchem, Houston, TX, USA) or vehicle (VEH) via intraperitoneal injection. Sham-loaded age-matched controls were euthanized at 0 or 28 days (n=6/time point). Prior to euthanasia at 7, 14, 21, or 28 days post-injury, inflammatory protease activity in injured

and uninjured limbs was quantified using Fluorescence Reflectance Imaging (FRI). All procedures were approved by the UC Davis Institutional Animal Care and Use Committee. No animals were excluded from the study due to adverse effects.

PTOA Initiation by Non-Invasive ACL Rupture

Right hindlimbs underwent ACL injury by tibial compression overload as previously described [13, 26, 28]. Mice were anesthetized prior to injury using isoflurane inhalation. Mice were placed in a prone position, with right lower limbs held in place vertically by two compressive loading platens. A single dynamic axial compressive load at 1 mm/s was applied until ACL rupture via an electromagnetic materials testing machine (ElectroForce 3200, TA Instruments, New Castle, DE). Buprenorphine analgesia was administered immediately after injury (0.01 mg/kg). Mice were then allowed normal cage activity, or were subject to 7 days of hindlimb unloading.

Hindlimb Unloading and Reloading

Immediately post-injury, 56 mice were subject to hindlimb unloading via tail suspension as previously described [13, 29, 30]. During unloading, mice were housed individually in custom-built cages for tail suspension (Techshot, Inc., Greenville, IN). Cages were prepared with wire mesh flooring siting above absorbent material. Metal loops were attached using cyanoacrylate to tail bases while mice were still under anesthesia from ACL rupture. These loops were attached to a swivel allowing for 360° rotation, and mounted on a bar across the length of the cage. Mice were placed with heads down at approximately 30°, with hindlimbs unable to touch the floor of the cage. This enabled passive movement of the hindlimbs, without any weight bearing. Mice could navigate the cage freely using their forelimbs, and were given food, water, and nesting materials ad libitum. Mice underwent hindlimb unloading for 7 days, after which they were anesthetized via isoflurane inhalation, metal loops and swivels were removed from mouse tails using acetone, and mice were placed back into group housing in standard mouse cages for the remainder of the study.

Anti-Inflammatory Treatment with Celecoxib

Mice were randomly assigned to CXB and VEH groups. CXB was dissolved in sterile saline, 2% dimethyl sulfoxide (DMSO), 30% polyethylene glycol 300, and 5% Tween 80. Mice were administered 10 mg/kg of CXB daily, and the daily volume of VEH or CXB solution was 2 mL/kg. VEH and CXB solutions were prepared fresh daily. Mouse abdomens were sterilized with ethanol prior to each injection, and a new needle was used for every mouse to prevent infection. Treatments were administered *via* intraperitoneal injection, alternating sides of the body with every injection.

Fluorescence Reflectance Imaging (FRI) of Protease Activity

Hindlimbs were imaged using *in vivo* FRI for inflammatory protease activity as previously described [13, 31]. Briefly, mice were anesthetized using isoflurane inhalation and injected retro-orbitally with 2 nmol per 25 g mouse ProSense 680 (PerkinElmer, Waltham, MA) 24 hours prior to imaging. ProSense 680 is a fluorescent probe activated by the proteases plasmin, and cathepsins B, L, and S, which are highly active during inflammation [32, 33].

Images were taken 0, 7, 14, 21, and 28 days post-injury. Immediately prior to imaging, mice were anesthetized *via* isoflurane inhalation and a depilatory was used to remove hair from the ventral aspect of the hindlimbs. Mice were imaged individually in a 13.3 cm field of view in the imaging system (IVIS Spectrum, PerkinElmer). The excitation and emission filters were 680 ± 10 nm and 700 ± 10 nm, respectively, with 0.5 sec exposure time. Care was taken to position mice in similar positions to ensure even epi-illumination across the medial knee and femur for both injured and contralateral limbs. Ankles were taped down, and image processing and quantification were performed using the IVIS *Living Image* software. Fluorescence intensity was quantified as the total radiant efficiency (TRE; [photons/s]/[$\mu\text{W}/\text{cm}^2$]) of the signal within a region of interest (ROI), as previously described [13, 31]. The ROI was a circle of radius 0.35 cm placed over the knee on a grayscale photograph of the mice to prevent bias from the fluorescent signal. Hindlimbs were collected post-imaging and fixed in 4% paraformaldehyde for 5–7 days, followed by preservation in 70% ethanol in preparation for μCT analysis.

Micro-Computed Tomography Analysis of Epiphyseal Trabecular Bone and Mineralized Osteophyte Volume

Whole knee joints were scanned using μCT (SCANCO μCT 35, Brüttisellen, Switzerland) to determine total mineralized osteophyte volume, as well as epiphyseal trabecular bone microstructure and apparent bone mineral density (aBMD). Scans were performed according to rodent bone structure analysis guidelines (X-ray tube potential = 55kVp, intensity = 114 μA , 10 μm isotropic nominal voxel size, integration time = 900ms) [34]. The bone tissue global threshold was set to 567 mg HA/cm³. Subchondral trabecular bone was analyzed at all time points at the distal femoral epiphysis. ROI contours were drawn to include all trabecular bone enclosed by the growth plate. Trabecular bone volume fraction (BV/TV), trabecular thickness (Tb.Th), and other microstructural outcomes were measured using the manufacturer's analysis tool.

Mineralized osteophyte volume was investigated starting at day 14 post-injury *via* μCT [28]. Total mineralized osteophyte volume was defined using previous methodology [28]. Briefly, ROI contours were drawn around all patella, fabellae, and meniscal mineralized tissues, as well as heterotopic mineralized tissue attached to the distal femur and proximal tibia. Contralateral limb patella, fabellae, and meniscal mineralized tissue were also measured. Total mineralized osteophyte volume was calculated as the difference in bone volume between injured and contralateral limbs.

Histological Assessment of Joint Degeneration and Synovitis

Whole-joint histology was used to evaluate articular cartilage and joint degeneration, and to quantify synovitis. After fixation, knee joints were decalcified using 0.5 M EDTA (pH 7.3) until endpoint determination by x-ray (Carestream In vivo FX-MS, Bruker Imaging), and processed for standard paraffin embedding. Sagittal 6 μm sections were cut across the medial aspect of the knee joint, and were stained with Safranin O/Fast Green (SafO/FG). Sections were qualitatively evaluated for articular cartilage degradation and overall joint degeneration and pathology. Synovitis was graded using a 6-point scoring system based on synovial thickness and cell density as previously described [35]. Slides from all mice were

graded independently by 3 readers at both the anterior and posterior aspect of the joint, and reader scores were averaged for each mouse. Readers were blinded to experimental groups during grading.

Statistical Analysis

Protease activity (FRI), osteophyte μ CT data, and synovitis grading were analyzed with 2-way ANOVA at each time point, stratified by treatment group (CXB or VEH), and ambulation (HLU or GC) using JMP 12 software (SAS Institute, Inc., Cary, NC). Post-hoc analyses were carried out by the Tukey-Kramer test. For trabecular bone μ CT data, we analyzed (longitudinal and paired) observations together for each outcome via a mixed effects model that accounted for repeated measurements (and resulting correlation) from the same mouse. We allowed a random intercept for each mouse, along with the 4 categorical covariates: injury status, treatment (CXB or VEH), ambulation (GC or HLU) and follow-up time. All data were tested for normality, and all p-values from different tests for normality were >0.15 (e.g., $p=0.38$ for Shapiro-Wilk test), which provides insufficient evidence to reject the assumption of normality. The probability plot and box plot also support the assumption that the data are reasonably bell-shaped. All data are presented as mean \pm standard deviation and/or 95% confidence interval. Significance was defined as $p<0.05$ for all tests; we did not adjust for multiple testing.

Results

Fluorescence Reflectance Imaging (FRI) of Protease Activity

FRI analysis of protease activity revealed that unloading post-injury reduced the inflammatory protease activity during the unloading period, but this reduction was not sustained during subsequent reloading (Fig. 2). At 7 days post-injury, knees from GC mice displayed 83% ($p<0.001$) and 63% ($p<0.001$) increases in TRE compared to uninjured mice for VEH and CXB, respectively. At this same time point, knees from HLU mice displayed 22% ($p=0.021$) and 30% ($p=0.001$) reductions in TRE compared to GC VEH and CXB mice, respectively. TRE of knees from HLU and GC mice was decreased at later time points (day 14–28) compared with day 7; no significant differences were detected relative to uninjured mice at these later time points. No significant differences were observed between HLU and GC mice, or between VEH and CXB mice at days 14–28.

Epiphyseal Trabecular Bone

MicroCT analysis revealed that BV/TV, Tb.Th, and other microstructural outcomes were decreased after injury in all treatment and ambulation groups (Fig. 3, Supplemental Table 1). At 7 days post-injury (the end of the hindlimb unloading period), the injured limb of GC-VEH mice exhibited a 22% lower BV/TV relative to baseline. This was significantly greater than in HLU-VEH mice, which exhibited a 15% lower BV/TV. Similarly, GC-CXB mice exhibited a 22% decrease in BV/TV, while HLU-CXB mice exhibited only a 14% decrease ($p=0.077$). At the same time point, contralateral limbs of GC mice exhibited 4–6% decreases in BV/TV relative to baseline, while contralateral limbs of HLU mice exhibited 7–8% decreases (regardless of treatment). At 14 days post-injury (7 days of reloading), GC-CXB mice still exhibited a 26% lower BV/TV than baseline, which was significantly greater than

the 18% decrease in HLU-CXB mice; no differences were observed between GC-VEH and HLU-VEH mice at this time point. Additionally, at day 14 Tb.N was significantly greater and Tb.Sp was significantly lower in HLU mice compared to GC mice (Supplemental Table 1). At later time points, no significant differences were observed between GC and HLU mice for any microstructural outcomes regardless of treatment. However, bone tissue mineral density (TMD) was significantly decreased in CXB mice compared to VEH mice at day 14 and day 21, and BV/TV and apparent BMD were significantly lower in CXB mice compared to VEH mice at day 28 (Supplemental Table 1).

Mineralized Osteophyte Volume

Mineralized osteophyte volume increased over time in all experimental groups, and was considerably reduced by HLU and CXB treatment (Fig. 4). Mineralized osteophytes were detectable with μ CT by 14 days post-injury, though osteophyte volumes were not significantly different between any experimental groups at this time point. At 21 days post-injury, HLU mice had 36% and 46% less mineralized osteophyte volume for VEH and CXB groups, respectively, compared to GC mice. Osteophyte volume in GC-VEH mice increased by 109% between day 21 and day 28 post-injury, and osteophyte volume of HLU-VEH mice remained 46% lower than that of GC-VEH mice at day 28. GC-CXB and HLU-CXB mice had similar osteophyte volume at day 28, and both groups had significantly lower osteophyte volume than GC-VEH mice (-30% for GC-CXB mice, -35% for HLU-CXB mice).

Histological Assessment of Synovitis

Synovitis was observed in injured joints by 7 days post-injury, but was significantly reduced in HLU mice relative to GC mice at this time point (Fig. 5). For example, at 7 days post-injury, mean synovitis grade for HLU-VEH mice was 2.48 ± 0.83 (95% confidence interval: 1.71–3.24), compared to 4.97 ± 0.46 (95% confidence interval: 4.49–5.46) for GC-VEH mice ($p < 0.001$). CXB treatment alone was not able to significantly reduce synovitis in GC mice at this time point, and CXB treatment in HLU mice was less effective at reducing synovitis than HLU alone (3.40 ± 0.53 mean synovitis score (95% confidence interval: 2.92–3.89) for HLU-CXB mice; $p = 0.028$). No significant differences were observed between VEH and CXB treated mice at later time points during reloading.

Histological Assessment of Joint Degeneration

Histological assessment revealed that HLU mice displayed clear slowing of PTOA progression, even after returning to cage activity (Fig. 6). Following ACL injury, the articulation of the distal femur of GC mice translated posteriorly relative to the proximal tibia and the posterior horn of the medial meniscus was dislocated anteriorly, resulting in considerable erosion of articular cartilage on the femoral condyle and posterior tibial plateau by day 14 post-injury. Additionally, considerable chondro/osteophyte formation was evident at the anterior-medial femur, the anterior horn of the medial meniscus, and the posterior-medial tibia. In contrast, the medial meniscus of HLU mice remained intact throughout the study period, and knee joints maintained the normal articulation between the femur and tibia. Chondrophyte formation was present in HLU mice, but to a lesser extent than in GC mice. By day 28, GC mice displayed well-developed osteophytes in the anterior-medial femur, anterior medial meniscus, and posterior-medial tibia, and severe

articular cartilage erosion was apparent in the posterior tibial plateau and femoral condyle, reaching through the zone of calcified cartilage. In contrast, HLU mice at day 28 displayed reduced osteophyte size, and the posterior tibial plateau displayed cartilage erosion, but over a smaller area and to a less severe degree than in GC mice. No apparent differences in the severity of articular cartilage degradation or joint degeneration were observed between CXB-treated and VEH-treated mice for either GC or HLU groups.

Discussion

In this study, we examined how early mechanical unloading and NSAID treatment after ACL rupture influenced subsequent PTOA progression. We found that unloading, but not CXB treatment, significantly reduced protease activity and synovitis during the unloading period, and was able to partially protect against early epiphyseal trabecular bone loss. However, protease activity, synovitis, and trabecular bone microstructure returned to the level of GC mice with reloading at later time points. Hindlimb unloading for 7 days post-injury led to longer-term impacts on osteophyte development, as did CXB administration, and early unloading protected the joint from meniscal dislocation and slowed the degeneration of articular cartilage. These results support our hypothesis that unloading during the early phase post-injury reduces subsequent osteophyte and PTOA progression, but do not support the hypothesis that CXB treatment would lead to reduced protease activity and further reduce osteophyte and PTOA development.

Traumatic joint injuries cause a temporally-dependent adaption response that includes an “early phase” characterized by cell death/apoptosis and inflammation, an “intermediate phase” with both catabolic and anabolic processes, and a “late phase” of repair, remodeling, and matrix formation [12, 36]. The surge of inflammatory cytokines and degradative enzymes such as cathepsin proteases and matrix metalloproteinases (MMPs) during the early phase can initiate degeneration of articular cartilage and subchondral bone [6, 12, 37–42], and put the injured joint on a trajectory toward developing PTOA. Unloading of the injured joint during the early phase may decrease joint inflammation and protease activity [27, 43–45], reduce joint pain and aggravation of injured joint tissues, and diminish early “wear and tear” due to joint instability and altered joint biomechanics [46]. However, while some amount of unloading may have the potential to reduce OA development, long-term immobilization can have a degenerative effect on the joint and lead to OA-like changes, even in uninjured limbs [47].

Our previous study investigating the effect of HLU in mice following non-invasive knee injury found that knee injury in GC mice resulted in ~29% decrease in epiphyseal trabecular bone volume (BV/TV) relative to uninjured mice at 7 days post-injury, and both injured and uninjured HLU mice exhibited comparable magnitudes of bone loss in both limbs (–20–29%) [29]. In comparison, the current study found significantly greater loss of trabecular bone volume in injured GC joints (–22%) compared to injured HLU joints (–15–16%) in both VEH and CXB-treated mice. Another of our studies found that HLU following knee injury reduced protease activity and inflammatory cytokine expression, and reduced the formation of chondrocytes in the injured joint during unloading [27], consistent with the results of the current study. However, neither of these previous studies investigated these

processes during subsequent reloading. The current study is the first to show that during reloading, protease activity, synovitis, and epiphyseal trabecular bone microstructure return to GC values by 14–21 days post-injury (7–14 days of reloading), while reductions in osteophyte formation and PTOA progression are observed until at least 28 days post-injury.

In the current study, CXB treatment did not have a significant effect on early protease activity or synovitis post-injury, but did affect osteophyte formation at 28 days post-injury. Previous work examining osteophyte development in ankylosing spondylitis found that chronic inflammation led to tissue degeneration, which in turn altered biomechanics and spurred osteophyte formation [48]. Other work suggests that inflammation may play a more direct role in osteophyte development: synovial macrophages have been found to be crucial in osteophyte formation, and S100A9-knockout mice, which have inhibited inflammatory synovitis, showed reduced osteophyte size (S100A9 is a protein released by activated macrophages that contributes to synovitis during OA) [49–51]. The relationship between osteophyte formation and inflammation is not well understood, which may be partially due to the difficulty in separating the effects of mechanical instability from post-injury or chronic inflammation.

Celecoxib is a cyclooxygenase-2 (COX-2) specific inhibitor that impairs bone formation after fracture, as well as normal skeletal function [52–55]. COX-1 and COX-2 are targets for most NSAIDs, and are responsible for converting arachidonic acid to prostaglandins at the start of many inflammatory cascades. NSAIDs that target COX-1 and –2 have been shown to inhibit fracture healing in a rat fracture model, and NSAID use was correlated with a higher incidence of non-unions in femur fracture patients [53, 56]. Additionally, COX-2 inhibition prevented tibial trabecular bone restoration during reloading following a period of unloading in mice [57]. In the current study, CXB treatment inhibited osteophyte development and led to reduced epiphyseal trabecular bone tissue mineral density, apparent BMD, and BV/TV at the day 28 time point. These results are consistent with previous studies; however, CXB is an anti-inflammatory drug, and our results did not indicate a decrease in protease activity or synovitis with CXB treatment. This may be because inhibition of COX-2 can lead to activation of other, compensatory, inflammatory pathways [58, 59]; we did not directly measure COX-2 activity or prostaglandin E2 (PGE₂) levels, which could have provided a more direct measurement of CXB efficacy. It is also possible that CXB treatment was not able to efficiently slow PTOA due to the rapidly progressing and severe OA that results from non-invasive ACL rupture in mice. CXB treatment in a slower progressing and less severe OA model such as destabilization of the medial meniscus (DMM) may be more effective at mitigating inflammation and slowing PTOA progression, though DMM and similar methods require invasive surgical procedures that could themselves initiate inflammation and tissue degradation.

This study has limitations that must be acknowledged in interpreting these results. Osteophyte volume was examined using μ CT, but this does not include early chondrophytes, which are not mineralized. Chondrophytes provide the blueprint for later mineralization into osteophytes, and differences in early chondrophyte formation may explain much of the later differences in the development of mature osteophytes after CXB treatment and/or HLU. Additionally, histological assessment of joints was used to qualitatively examine

chondrocyte formation, degeneration of knee tissues, and overall PTOA development. However, quantitative analysis may provide additional data regarding chondro/osteocyte size and PTOA progression, though this can be somewhat limited due to the narrow focus on articular cartilage. A more in-depth immunohistochemical characterization could also help determine changes in cell viability/apoptosis, changes in proteinase activity, or other molecular level effects that could explain the effects of HLU and CXB. We are currently only able to speculate about the cellular mechanisms driving many these effects, and future work will be needed to characterize many of the underlying processes. Another potential limitation of this study is the use of CXB, a specific COX-2 inhibitor. Using a non-specific COX inhibitor that affects both COX-1 and COX-2 may have been more clinically relevant and provided a more thorough inhibition of the post-injury inflammatory response. Furthermore, we did not include a control group of uninjured mice treated with CXB. This would have allowed for a more thorough understanding of the effects of CXB in the absence of injury. In this study, we also only evaluated PTOA through 28 days of injury in mice. In previous work, we showed that osteocyte growth slows after 28 days, but longer time points would have provided greater information regarding the long-term development of PTOA [13]. We also only used young, skeletally mature, female mice in this study; including other sexes and ages may have yielded additional results to determine the influence of these factors toward osteocyte and PTOA development. Female mice were used in this study due to concerns about fighting in male mice, particularly when mice are returned to group housing after one week of hindlimb unloading. Fighting may also introduce high variability in activity level and mechanical loading of the joint that could affect the rate of joint degeneration [60].

The results of this study are relevant to orthopaedic practice and treatment of traumatic joint injuries because there is currently no clinical consensus on recommendations for joint loading (exercise/walking) or unloading (rest/disuse) in the Early Phase following injury. Most physicians will recommend rest, ice, compression, and elevation (RICE) of the injured joint during the first few days following injury, along with anti-inflammatory medications to control swelling and pain. Moderate activity is often recommended soon after injury to maintain muscle mass and strength, and to maintain joint range of motion. This is thought to be important because mechanical unloading causes atrophy of subchondral bone and muscle in the unloaded limb, and maintaining muscle mass and function, joint range of motion, and subchondral bone structure are clinically desirable to improve the success of surgical repairs and post-surgical outcomes [61–66]. However, excess loading of the injured joint during the Early Phase may exacerbate inflammation and aggravate the injured joint tissues. Therefore, there is a potential tradeoff between preventing long-term joint degeneration and maintaining short-term muscle/bone structure and joint function. The findings of this study show that unloading during the Early Phase can diminish early protease activity and synovitis in the joint, and may slow mechanical damage to joint structures and lessen osteocyte formation, which could have long-lasting benefits to joint health.

Conclusions:

In this study, we investigated how biomechanical and anti-inflammatory treatments during the early phase post-injury influence osteocyte formation and PTOA progression. Our

results suggest that early unloading in particular may have a beneficial long-term effects on osteophyte formation and OA progression. However, further study is needed to clarify the mechanism by which unloading is able to preserve joint health, and to optimize the biomechanical environment for slowing or preventing PTOA. Increasing knowledge of biomechanical therapies for slowing osteophyte formation and PTOA progression may translate into future innovations for more effective treatment of joint injuries, improving the lives of the millions affected by this debilitating disease.

Supplementary Material

Refer to Web version on PubMed Central for supplementary material.

Acknowledgements:

Research reported in this publication was supported by the National Institute of Arthritis and Musculoskeletal and Skin Diseases, part of the National Institutes of Health, under Award Number AR075013. The content is solely the responsibility of the authors and does not necessarily represent the official views of the National Institutes of Health. The funding body was not involved with design, collection, analysis, or interpretation of data; or in the writing of the manuscript. MEM and GGL contribution were carried under the auspices of the USDOE by LLNL (DE-AC52-07NA27344).

References

1. Brown TD, Johnston RC, Saltzman CL, et al. , Posttraumatic osteoarthritis: a first estimate of incidence, prevalence, and burden of disease. *J Orthop Trauma*, 2006. 20(10): p. 739–44. [PubMed: 17106388]
2. Lawrence RC, Felson DT, Helmick CG, et al. , Estimates of the prevalence of arthritis and other rheumatic conditions in the United States. Part II. *Arthritis Rheum*, 2008. 58(1): p. 26–35. [PubMed: 18163497]
3. Dare D and Rodeo S, Mechanisms of post-traumatic osteoarthritis after ACL injury. *Curr Rheumatol Rep*, 2014. 16(10): p. 448. [PubMed: 25182676]
4. Racine J and Aaron RK, Post-traumatic osteoarthritis after ACL injury. *R I Med J* (2013), 2014. 97(11): p. 25–8.
5. Wang LJ, Zeng N, Yan ZP, et al. , Post-traumatic osteoarthritis following ACL injury. *Arthritis Res Ther*, 2020. 22(1): p. 57. [PubMed: 32209130]
6. Lohmander LS, Englund PM, Dahl LL, et al. , The long-term consequence of anterior cruciate ligament and meniscus injuries: osteoarthritis. *Am J Sports Med*, 2007. 35(10): p. 1756–69. [PubMed: 17761605]
7. Badlani JT, Borrero C, Golla S, et al. , The effects of meniscus injury on the development of knee osteoarthritis: data from the osteoarthritis initiative. *Am J Sports Med*, 2013. 41(6): p. 1238–44. [PubMed: 23733830]
8. Punzi L, Galozzi P, Luisetto R, et al. , Post-traumatic arthritis: overview on pathogenic mechanisms and role of inflammation. *RMD Open*, 2016. 2(2): p. e000279. [PubMed: 27651925]
9. McKinley TO, Borrelli J Jr., D’Lima DD, et al. , Basic science of intra-articular fractures and posttraumatic osteoarthritis. *J Orthop Trauma*, 2010. 24(9): p. 567–70. [PubMed: 20736796]
10. Schenker ML, Mauck RL, Ahn J, et al. , Pathogenesis and prevention of posttraumatic osteoarthritis after intra-articular fracture. *J Am Acad Orthop Surg*, 2014. 22(1): p. 20–8. [PubMed: 24382876]
11. Goldring SR and Goldring MB, Clinical aspects, pathology and pathophysiology of osteoarthritis. *J Musculoskelet Neuronal Interact*, 2006. 6(4): p. 376–8. [PubMed: 17185832]
12. Anderson DD, Chubinskaya S, Guilak F, et al. , Post-traumatic osteoarthritis: Improved understanding and opportunities for early intervention. *J Orthop Res*, 2011. 29(6): p. 802–9. [PubMed: 21520254]

13. Hsia AW, Emami AJ, Tarke FD, et al. , Osteophytes and fracture calluses share developmental milestones and are diminished by unloading. *J Orthop Res*, 2017.
14. Williams JM and Brandt KD, Temporary immobilisation facilitates repair of chemically induced articular cartilage injury. *J Anat*, 1984. 138 (Pt 3): p. 435–46. [PubMed: 6735906]
15. Williams JM and Brandt KD, Immobilization ameliorates chemically-induced articular cartilage damage. *Arthritis Rheum*, 1984. 27(2): p. 208–16. [PubMed: 6696774]
16. Palmoski MJ and Brandt KD, Immobilization of the knee prevents osteoarthritis after anterior cruciate ligament transection. *Arthritis Rheum*, 1982. 25(10): p. 1201–8. [PubMed: 7138593]
17. Haapala J, Arokoski JP, Ronkko S, et al. , Decline after immobilisation and recovery after remobilisation of synovial fluid IL1, TIMP, and chondroitin sulphate levels in young beagle dogs. *Ann Rheum Dis*, 2001. 60(1): p. 55–60. [PubMed: 11114283]
18. Brandt KD, Response of joint structures to inactivity and to reloading after immobilization. *Arthritis Rheum*, 2003. 49(2): p. 267–71. [PubMed: 12687522]
19. Palmoski MJ and Brandt KD, Running inhibits the reversal of atrophic changes in canine knee cartilage after removal of a leg cast. *Arthritis Rheum*, 1981. 24(11): p. 1329–37. [PubMed: 7317111]
20. Zweers MC, de Boer TN, van Roon J, et al. , Celecoxib: considerations regarding its potential disease-modifying properties in osteoarthritis. *Arthritis Res Ther*, 2011. 13(5): p. 239. [PubMed: 21955617]
21. Taketa T, Sakai A, Tanaka S, et al. , Selective cyclooxygenase-2 inhibitor prevents reduction of trabecular bone mass in collagen-induced arthritic mice in association with suppression of RANKL/OPG ratio and IL-6 mRNA expression in synovial tissues but not in bone marrow cells. *J Bone Miner Metab*, 2008. 26(2): p. 143–51. [PubMed: 18301970]
22. Park SY, Lee YS, Lee SY, et al. , Multitarget-based cotreatment with cilostazol and celecoxib synergistically suppresses collagen-induced arthritis in mice by enhancing interleukin-10 expression. *Int Immunopharmacol*, 2019. 73: p. 461–470. [PubMed: 31170675]
23. Tu M, Yang M, Yu N, et al. , Inhibition of cyclooxygenase-2 activity in subchondral bone modifies a subtype of osteoarthritis. *Bone Res*, 2019. 7: p. 29. [PubMed: 31666999]
24. Tellegen AR, Rudnik-Jansen I, Pouran B, et al. , Controlled release of celecoxib inhibits inflammation, bone cysts and osteophyte formation in a preclinical model of osteoarthritis. *Drug Deliv*, 2018. 25(1): p. 1438–1447. [PubMed: 29890922]
25. Jilka RL, The relevance of mouse models for investigating age-related bone loss in humans. *J Gerontol A Biol Sci Med Sci*, 2013. 68(10): p. 1209–17. [PubMed: 23689830]
26. Christiansen BA, Anderson MJ, Lee CA, et al. , Musculoskeletal changes following non-invasive knee injury using a novel mouse model of post-traumatic osteoarthritis. *Osteoarthritis Cartilage*, 2012. 20(7): p. 773–82. [PubMed: 22531459]
27. Hsia AW, Emami AJ, Tarke FD, et al. , Osteophytes and fracture calluses share developmental milestones and are diminished by unloading. *J Orthop Res*, 2018. 36(2): p. 699–710. [PubMed: 29058776]
28. Hsia AW, Anderson MJ, Heffner MA, et al. , Osteophyte formation after ACL rupture in mice is associated with joint restabilization and loss of range of motion. *J Orthop Res*, 2017. 35(3): p. 466–473. [PubMed: 27031945]
29. Anderson MJ, Diko S, Baehr LM, et al. , Contribution of mechanical unloading to trabecular bone loss following non-invasive knee injury in mice. *J Orthop Res*, 2016. 34(10): p. 1680–1687. [PubMed: 26826014]
30. Warden SJ, Galley MR, Richard JS, et al. , Reduced gravitational loading does not account for the skeletal effect of botulinum toxin-induced muscle inhibition suggesting a direct effect of muscle on bone. *Bone*, 2013. 54(1): p. 98–105. [PubMed: 23388417]
31. Satkunanathan PB, Anderson MJ, De Jesus NM, et al. , In vivo fluorescence reflectance imaging of protease activity in a mouse model of post-traumatic osteoarthritis. *Osteoarthritis Cartilage*, 2014. 22(10): p. 1461–9. [PubMed: 25278057]
32. Conus S and Simon HU, Cathepsins: key modulators of cell death and inflammatory responses. *Biochem Pharmacol*, 2008. 76(11): p. 1374–82. [PubMed: 18762176]

33. Goergen CJ, Azuma J, Barr KN, et al. , Influences of aortic motion and curvature on vessel expansion in murine experimental aneurysms. *Arterioscler Thromb Vasc Biol*, 2011. 31(2): p. 270–9. [PubMed: 21071686]
34. Bouxsein ML, Boyd SK, Christiansen BA, et al. , Guidelines for assessment of bone microstructure in rodents using micro-computed tomography. *J Bone Miner Res*, 2010. 25(7): p. 1468–86. [PubMed: 20533309]
35. Lewis JS, Hembree WC, Furman BD, et al. , Acute joint pathology and synovial inflammation is associated with increased intra-articular fracture severity in the mouse knee. *Osteoarthritis Cartilage*, 2011. 19(7): p. 864–73. [PubMed: 21619936]
36. Lotz MK and Kraus VB, New developments in osteoarthritis. Posttraumatic osteoarthritis: pathogenesis and pharmacological treatment options. *Arthritis Res Ther*, 2010. 12(3): p. 211. [PubMed: 20602810]
37. Madry H, Luyten FP, and Facchini A, Biological aspects of early osteoarthritis. *Knee Surg Sports Traumatol Arthrosc*, 2012. 20(3): p. 407–22. [PubMed: 22009557]
38. Goldring MB and Goldring SR, Osteoarthritis. *Journal of Cellular Physiology*, 2007. 213(3): p. 626–634. [PubMed: 17786965]
39. Kurz B, Lemke AK, Fay J, et al. , Pathomechanisms of cartilage destruction by mechanical injury. *Ann Anat*, 2005. 187(5–6): p. 473–85. [PubMed: 16320827]
40. Fitzgerald JB, Jin M, Dean D, et al. , Mechanical compression of cartilage explants induces multiple time-dependent gene expression patterns and involves intracellular calcium and cyclic AMP. *J Biol Chem*, 2004. 279(19): p. 19502–11. [PubMed: 14960571]
41. Brophy RH, Rai MF, Zhang Z, et al. , Molecular analysis of age and sex-related gene expression in meniscal tears with and without a concomitant anterior cruciate ligament tear. *J Bone Joint Surg Am*, 2012. 94(5): p. 385–93. [PubMed: 22362494]
42. Irie K, Uchiyama E, and Iwaso H, Intraarticular inflammatory cytokines in acute anterior cruciate ligament injured knee. *Knee*, 2003. 10(1): p. 93–6. [PubMed: 12649034]
43. Blomgran P, Blomgran R, Ernerudh J, et al. , A possible link between loading, inflammation and healing: Immune cell populations during tendon healing in the rat. *Sci Rep*, 2016. 6: p. 29824. [PubMed: 27405922]
44. Kohno S, Yamashita Y, Abe T, et al. , Unloading stress disturbs muscle regeneration through perturbed recruitment and function of macrophages. *J Appl Physiol (1985)*, 2012. 112(10): p. 1773–82. [PubMed: 22383511]
45. Grenon SM, Jeanne M, Aguado-Zuniga J, et al. , Effects of gravitational mechanical unloading in endothelial cells: association between caveolins, inflammation and adhesion molecules. *Sci Rep*, 2013. 3: p. 1494. [PubMed: 23511048]
46. Lafeber FP, Intema F, Van Roermund PM, et al. , Unloading joints to treat osteoarthritis, including joint distraction. *Curr Opin Rheumatol*, 2006. 18(5): p. 519–25. [PubMed: 16896294]
47. Langenskiold A, Michelsson JE, and Videman T, Osteoarthritis of the knee in the rabbit produced by immobilization. Attempts to achieve a reproducible model for studies on pathogenesis and therapy. *Acta Orthop Scand*, 1979. 50(1): p. 1–14. [PubMed: 425824]
48. Tseng HW, Pitt ME, Glant TT, et al. , Inflammation-driven bone formation in a mouse model of ankylosing spondylitis: sequential not parallel processes. *Arthritis Res Ther*, 2016. 18: p. 35. [PubMed: 26831337]
49. Blom AB, van Lent PL, Holthuysen AE, et al. , Synovial lining macrophages mediate osteophyte formation during experimental osteoarthritis. *Osteoarthritis Cartilage*, 2004. 12(8): p. 627–35. [PubMed: 15262242]
50. Schelbergen RF, de Munter W, van den Bosch MH, et al. , Alarmins S100A8/S100A9 aggravate osteophyte formation in experimental osteoarthritis and predict osteophyte progression in early human symptomatic osteoarthritis. *Ann Rheum Dis*, 2016. 75(1): p. 218–25. [PubMed: 25180294]
51. van Lent PL, Blom AB, Schelbergen RF, et al. , Active involvement of alarmins S100A8 and S100A9 in the regulation of synovial activation and joint destruction during mouse and human osteoarthritis. *Arthritis Rheum*, 2012. 64(5): p. 1466–76. [PubMed: 22143922]
52. Simon AM, Manigrasso MB, and O'Connor JP, Cyclo-oxygenase 2 function is essential for bone fracture healing. *J Bone Miner Res*, 2002. 17(6): p. 963–76. [PubMed: 12054171]

53. Simon AM and O'Connor JP, Dose and time-dependent effects of cyclooxygenase-2 inhibition on fracture-healing. *J Bone Joint Surg Am*, 2007. 89(3): p. 500–11. [PubMed: 17332098]
54. Lu LY, Loi F, Nathan K, et al. , Pro-inflammatory M1 macrophages promote Osteogenesis by mesenchymal stem cells via the COX-2-prostaglandin E2 pathway. *J Orthop Res*, 2017. 35(11): p. 2378–2385. [PubMed: 28248001]
55. O'Connor JP and Lysz T, Celecoxib, NSAIDs and the skeleton. *Drugs Today (Barc)*, 2008. 44(9): p. 693–709. [PubMed: 19137124]
56. Giannoudis PV, MacDonald DA, Matthews SJ, et al. , Nonunion of the femoral diaphysis. The influence of reaming and non-steroidal anti-inflammatory drugs. *J Bone Joint Surg Br*, 2000. 82(5): p. 655–8. [PubMed: 10963160]
57. Nakai K, Tanaka S, Sakai A, et al. , Cyclooxygenase-2 selective inhibition suppresses restoration of tibial trabecular bone formation in association with restriction of osteoblast maturation in skeletal reloading after hindlimb elevation of mice. *Bone*, 2006. 39(1): p. 83–92. [PubMed: 16487758]
58. Niederberger E, Tegeder I, Vetter G, et al. , Celecoxib loses its anti-inflammatory efficacy at high doses through activation of NF-kappaB. *FASEB J*, 2001. 15(9): p. 1622–4. [PubMed: 11427506]
59. Page TH, Turner JJ, Brown AC, et al. , Nonsteroidal anti-inflammatory drugs increase TNF production in rheumatoid synovial membrane cultures and whole blood. *J Immunol*, 2010. 185(6): p. 3694–701. [PubMed: 20713883]
60. Meakin LB, Sugiyama T, Galea GL, et al. , Male mice housed in groups engage in frequent fighting and show a lower response to additional bone loading than females or individually housed males that do not fight. *Bone*, 2013. 54(1): p. 113–7. [PubMed: 23356987]
61. Shelbourne KD and Gray T, Minimum 10-year results after anterior cruciate ligament reconstruction: how the loss of normal knee motion compounds other factors related to the development of osteoarthritis after surgery. *Am J Sports Med*, 2009. 37(3): p. 471–80. [PubMed: 19059893]
62. Eitzen I, Holm I, and Risberg MA, Preoperative quadriceps strength is a significant predictor of knee function two years after anterior cruciate ligament reconstruction. *Br J Sports Med*, 2009. 43(5): p. 371–6. [PubMed: 19224907]
63. Roe J, Pinczewski LA, Russell VJ, et al. , A 7-year follow-up of patellar tendon and hamstring tendon grafts for arthroscopic anterior cruciate ligament reconstruction: differences and similarities. *Am J Sports Med*, 2005. 33(9): p. 1337–45. [PubMed: 16002487]
64. Kraus VB, Feng S, Wang S, et al. , Subchondral bone trabecular integrity predicts and changes concurrently with radiographic and magnetic resonance imaging-determined knee osteoarthritis progression. *Arthritis Rheum*, 2013. 65(7): p. 1812–1821. [PubMed: 23576116]
65. Lewek M, Rudolph K, Axe M, et al. , The effect of insufficient quadriceps strength on gait after anterior cruciate ligament reconstruction. *Clin Biomech (Bristol, Avon)*, 2002. 17(1): p. 56–63.
66. Mauro CS, Irrgang JJ, Williams BA, et al. , Loss of extension following anterior cruciate ligament reconstruction: analysis of incidence and etiology using IKDC criteria. *Arthroscopy*, 2008. 24(2): p. 146–53. [PubMed: 18237697]

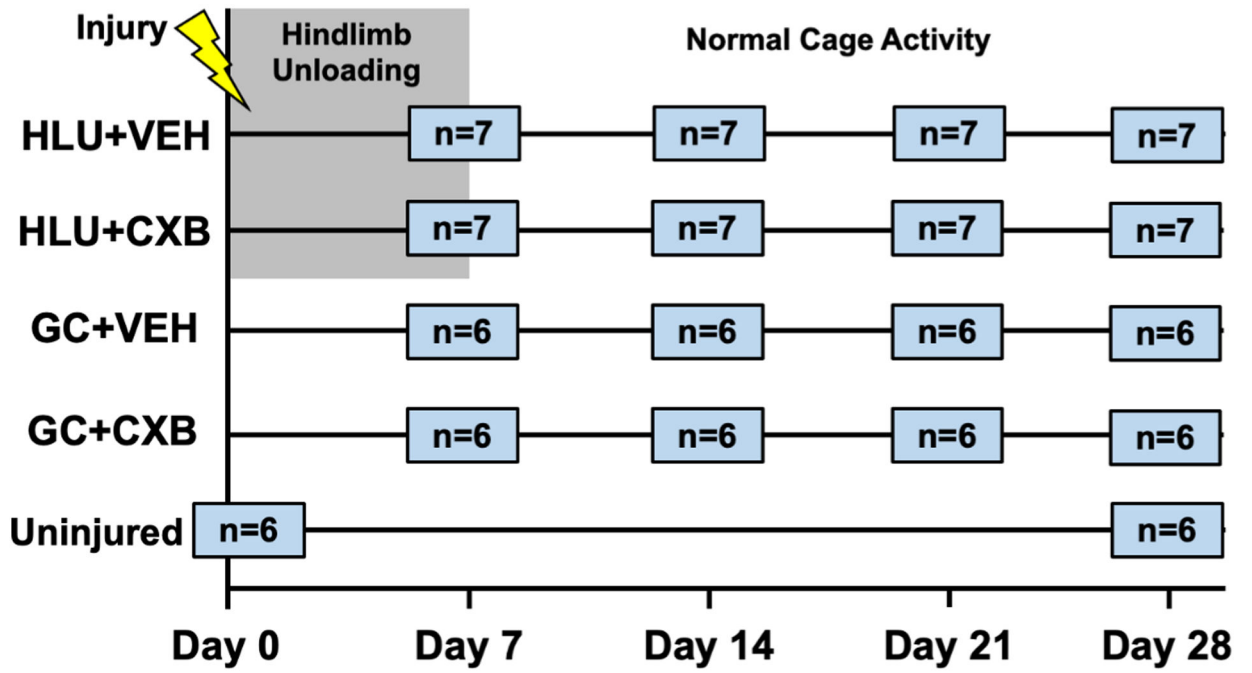


Figure 1:
Study design showing group sizes, terminal time points, and treatment groups.

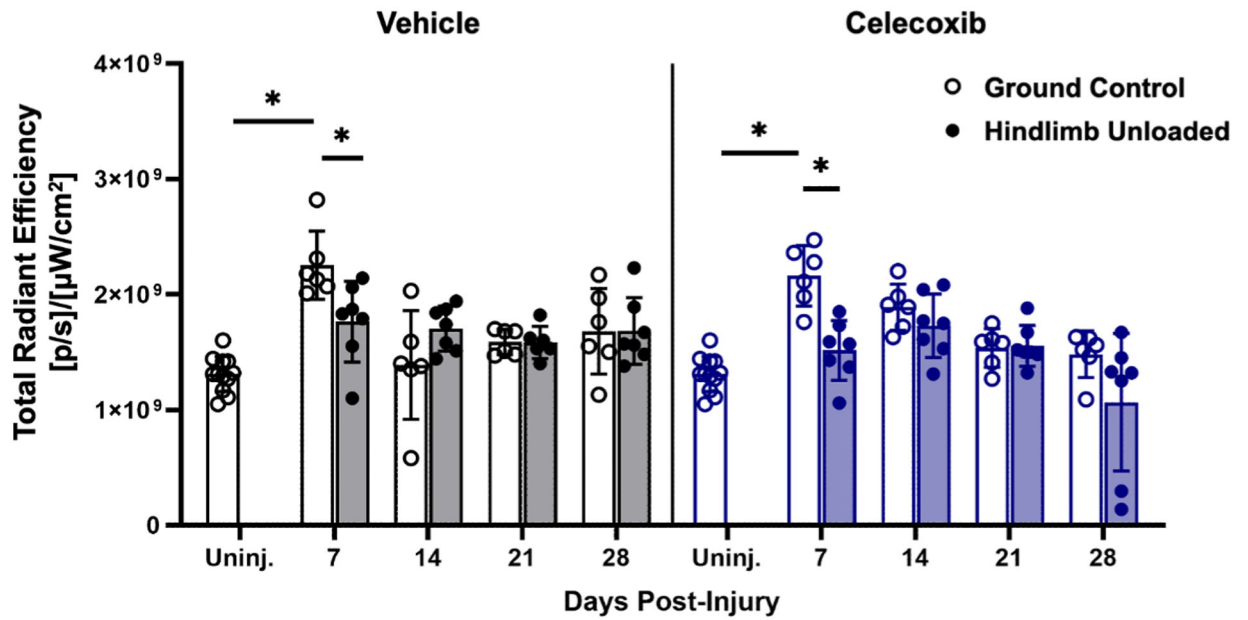


Figure 2:
Total Radiant Efficiency (TRE) as a measure for inflammatory protease activity in injured limbs in VEH (left) and CXB (right) treated mice. Hindlimb unloading decreased inflammatory protease activity at 7 days post-injury (during unloading), but this decrease was not observed at later time points during reloading. * $p < 0.05$

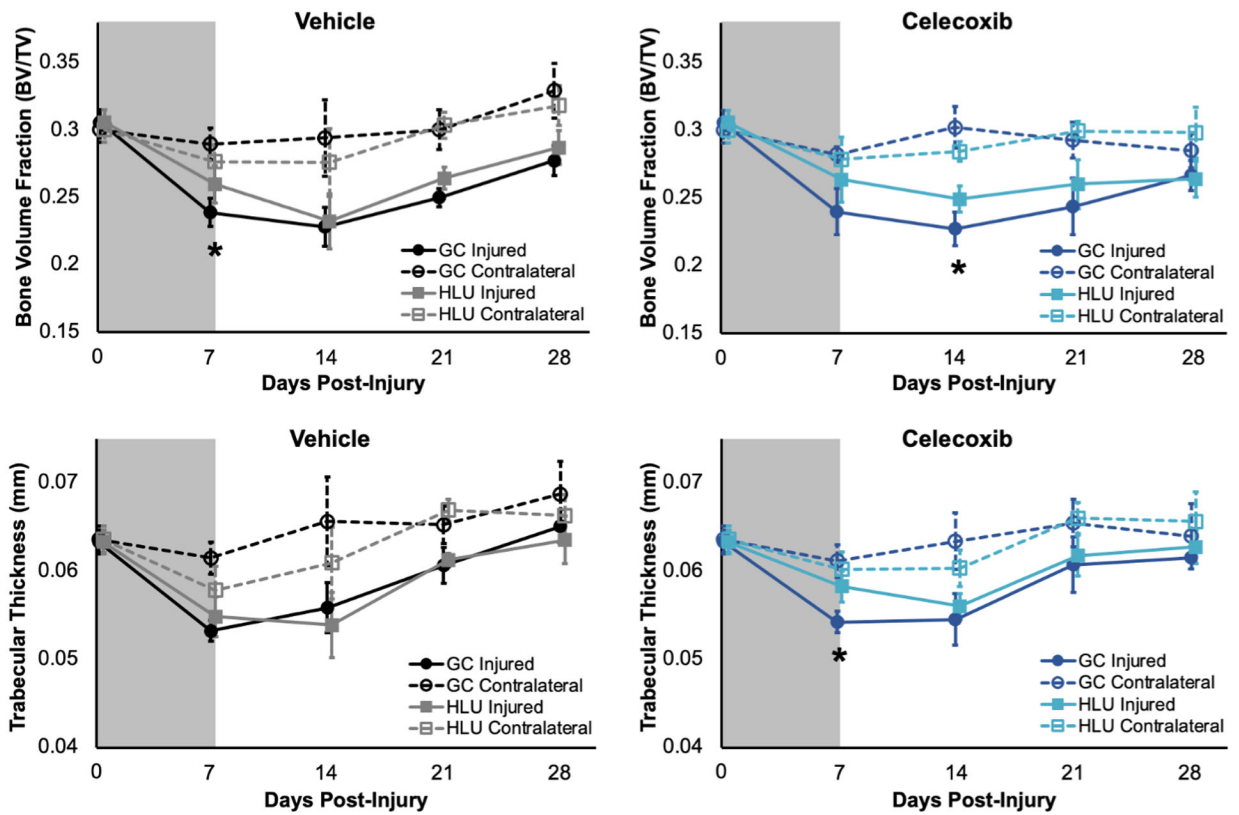


Figure 3:

Trabecular bone volume fraction (BV/TV) and trabecular thickness (Tb.Th) of distal femoral epiphyseal trabecular bone. Non-invasive ACL injury resulted in decreased trabecular bone volume in injured limbs, but unloading was able to partially prevent this bone loss. Differences in trabecular bone morphology between GC and HLU mice were not maintained at later time points during reloading. Gray background indicates the period of hindlimb unloading. Data presented as mean with 95% confidence interval. * Injured GC different from Injured HLU $p < 0.05$.

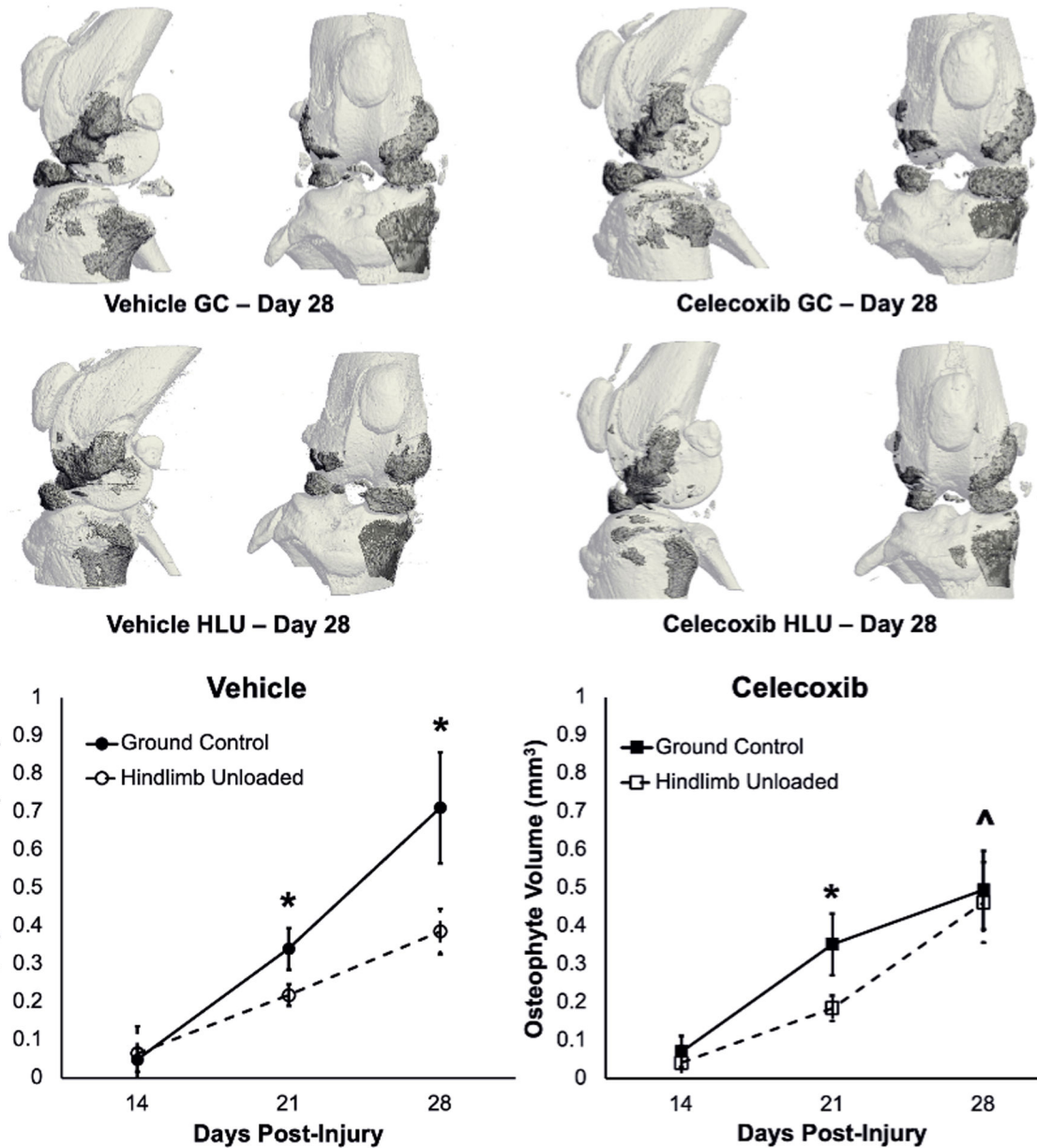


Figure 4. Mineralized osteophyte volume decreased with hindlimb unloading and CXB treatment at 21 and 28 days post-injury. ^ Both GC-CXB and HLU-CXB mice displayed reduced mineralized osteophyte volume compared to GC-VEH mice at 28 days post-injury. Data presented as mean with 95% confidence interval. * GC different from HLU $p < 0.05$.

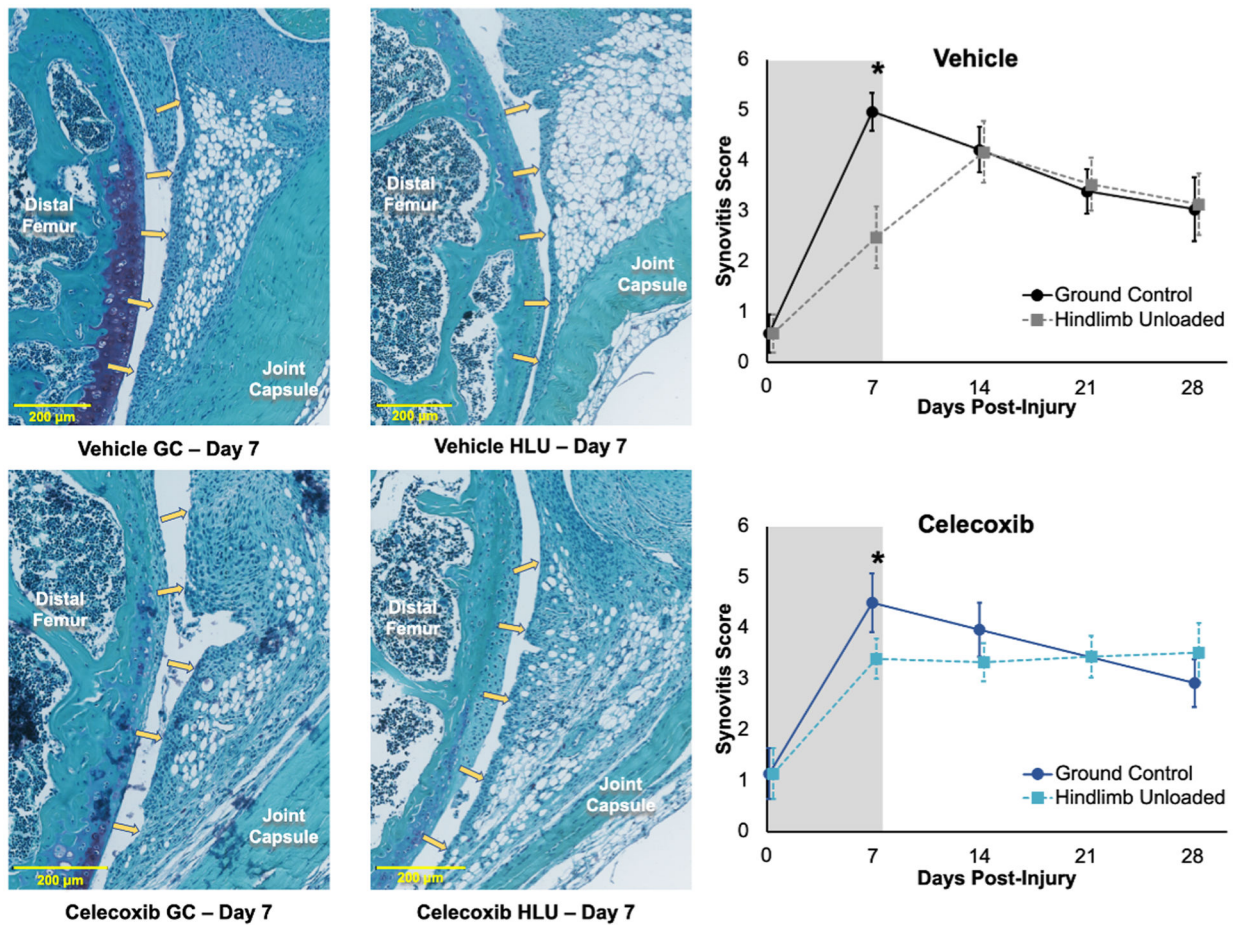


Figure 5.

(Left) Representative images of synovium (indicated with arrows) at the anterior aspect of injured knee joints at 7 days post-injury. (Right) Mean synovitis scores for VEH-treated mice (top) and CXB-treated mice (bottom). Hindlimb unloading reduced synovitis in both VEH- and CXB-treated mice relative to GC mice, though this was more effective in HLU-VEH mice. No differences in synovitis were observed at later time points (during reloading). Gray background indicates the period of hindlimb unloading. Data presented as mean with 95% confidence interval. * Injured GC different from Injured HLU $p < 0.05$.

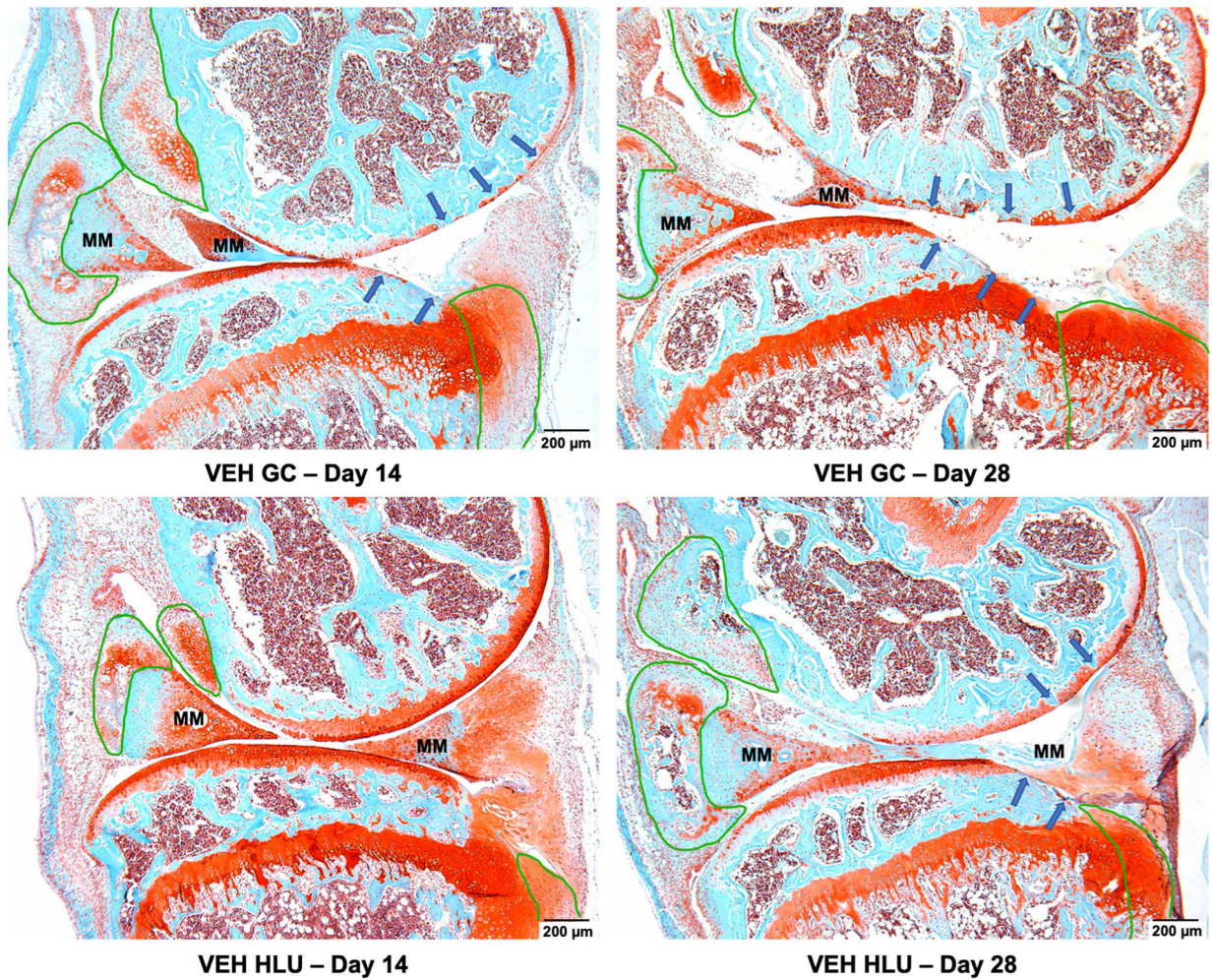


Figure 6. Representative histological sections of the medial articulation of VEH-treated mouse knee joints at day 14 and 28 post-injury. Knees of GC mice displayed considerable chondro/osteophyte formation (outlined in green) and articular cartilage erosion on the femoral condyle and posterior tibia (indicated with arrows). HLU prevented dislocation of the posterior horn of the medial meniscus (labelled MM), reduced chondro/osteophyte formation, and slowed articular cartilage erosion on both the tibia and femur. No apparent differences in the severity of articular cartilage degradation or joint degeneration were observed between CXB-treated and VEH-treated mice.